Lecture 10

The Cosmic Microwave Background

The cosmic microwave background (CMB) is an isotropic blackbody radiation field with temperature

$$T_{\rm CMB} = (2.726 \pm 0.001)\,{\rm K}. \tag{1}$$

A Bit of History

In the 1960's a group of physicists at Princeton University began to search for the presence of thermal radiation remaining from the "primordial fireball." Their research was directed by Robert Dicke, who by then had made contributions to a wide range of physics, including radar development and atomic theory, but focused now on gravitation theory. A member of that group, Jim Peebles, independently derived the results of Alpher and Herman [1]. Using microwave receiver technology that Dicke had developed twenty years earlier, called the Dicke radiometer, the Princeton group set about measuring this relic radiation on the roof of Guyot Hall in 1964. The experimental effort was led by Roll and Wilkinson [2]. As the Princeton group was commencing its measurements another New Jersey duo, Penzias and Wilson, had begun using a Dicke radiometer for radio astronomy. Battling an unknown noise contaminant, the pair had exhausted all avenues of reason, as they resorted to the sweeping of pigeon droppings inside their monstrous receiver horn. The Bell Labs researchers eventually made contact with the Princeton group which helped them understand their predicament. Penzias and Wilson had serendipitously discovered the cosmic microwave background, an incredibly uniform blackbody signal

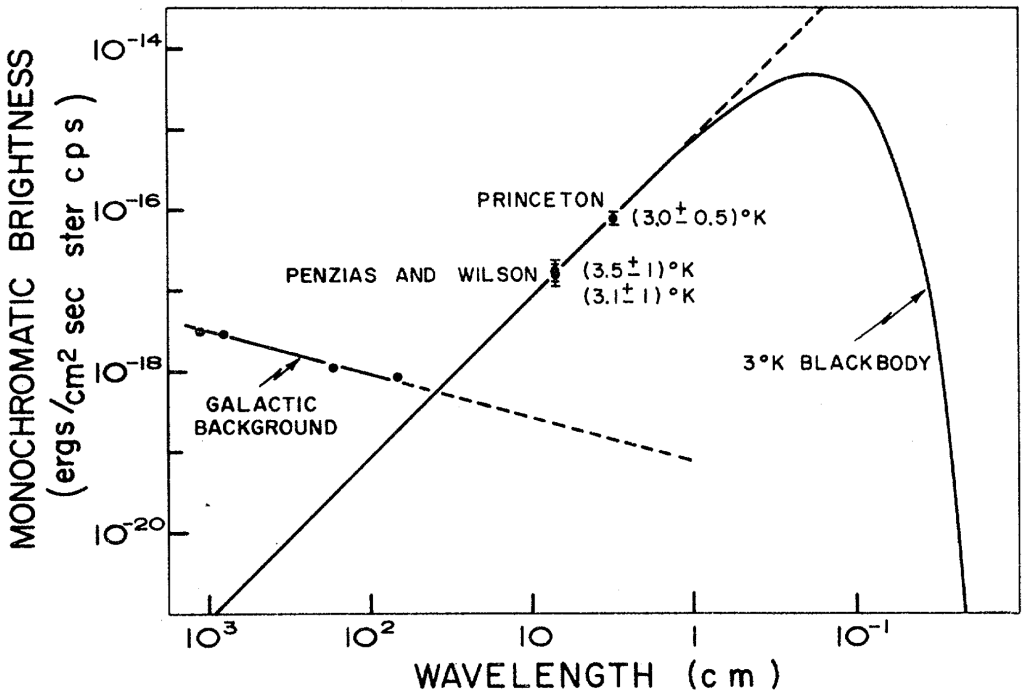

Figure 1: The results of the two New Jersey measurements, published in 1966 [4], showing intensity as a function of wavelength with a 3 K blackbody spectrum plotted for comparison. Both the Bell Labs (7.35 cm) and the Princeton measurement (3.2 cm) were performed safely within the Rayleigh-Jeans limit, almost two orders of magnitude below the peak value of a 3 K blackbody. Figure reproduced courtesy of P. J. E. Peebles.

coming from all directions on the sky [3]. Subsequent work by physicists at Princeton helped define the results and their theoretical implications [4, 5]. The discovery of the CMB brought the big bang universe to the forefront of modern physics.

Figure 1 shows the results from the first Bell Labs and Princeton measurements overlaid on a 3 K blackbody spectrum. Despite common belief, the 1964 Bell Labs measurements did not represent the first evidence for a uniform cosmic afterglow. The study of CN molecular spectra, published as early as 1940, suggested "a maximum effective temperature of interstellar space" of about 1–3 K [6, 7] and an excess temperature of space was reported during the commissioning of the Bell Labs receiver [8, 9]. Regardless of who should be acknowledged for the initial discovery, the study of this signal continued, and we now know that the CMB is almost a

perfect blackbody with temperature $T_{\rm CMB} = 2.726\,{\rm K}$ [10]. Its spectral radiance as a function of frequency, ν, follows the form

$$B(\nu) = \frac{2h\nu^3}{c^2}\frac{1}{\exp(h\nu/k_{\rm B}T) - 1}, \tag{2}$$

where h and $k_{\rm B}$ are Planck and Boltzmann constants respectively, T is the blackbody temperature, and c is the speed of light in vacuum.

Penzias' and Wilson's discovery of the cosmic microwave background, which later won them a Nobel prize, seeded the main bough of observational cosmology. Numerous experimental endeavors ensued, with efforts attempting to measure the uniformity [11] or spectral shape [12] of this fossil signal. Arguably the most famous of these early experiments is the Cosmic Background Explorer (*COBE*) satellite. The satellite was launched in 1989 with three instruments designed to measure different properties of the cosmic microwave background.

Using only 9 minutes of data spanning wavelengths of 1 cm to 0.5 mm, the FIRAS instrument measured a background radiation which was fit well by a 2.7 K blackbody spectrum [13]. During a 1992 meeting of the American Physical Society, measurements of CMB anisotropies were revealed, causing much stir in the scientific community. Publications of the main results followed in the Astrophysical Journal [14, 15]. After four years of observation, the coarse resolution DMR instrument had constructed a full sky image of the cosmic microwave background with fluctuation in the temperature of about ten parts per million.[1] This was, and continues to be, the strongest argument for isotropy and the Copernican principle (see Section 4). At this point, observational cosmology had been established as an avenue for

[1] Only the CMB dipole anisotropy had been measured before the DMR results.

answering fundamental questions about the nature of the universe. The hot big bang scenario was no longer contested.

1 Primordial Perturbations

The average density of our universe corresponds to a proton per cubic meter! Yet, this seemingly lifeless universe is able to facilitate the growth of galaxies, solar systems, and planets — structure as it is known to us. To explain this we invoke primordial density perturbations as quantum fluctuations of the inflaton (more on this during Lecture 11), or more generally as perturbations to the FLRW metric. We believe that perturbations, seeded during the very early universe, survive the transition from our speculative models of the embryonic universe to a largely uncontested hot and dense infant universe developing according to established laws of physics. We think that the perturbations are imprinted into the spectrum of the cosmic microwave background, and with proper care, can shed light on the early universe. By poking at the statistical properties of the CMB, we hope to learn something about the initial conditions of the universe.

On large scales, variation in the temperature of the CMB are affected by spatial curvature perturbations, Φ. On large scales, the CMB temperature anisotropies at some location on the sky, $\mathbf{n}$, are connected to the gravitational effects of density perturbations

$$\frac{\delta T}{T}(\mathbf{n}) = -\frac{1}{3}\Phi(\mathbf{n}), \tag{3}$$

where the stuff on the right hand side represents potential energy (see Sections 11.2–11.6 in B&G).

The time-development of variations in matter, photons, energy, etc., is described by the Friedmann and fluid equations. The important thing to note is that variations in photon and matter densities are coupled: Gravitational attractions in the photon-baryon plasma tend to form halos with infalling matter while increasing photon pressure impedes this process and erases anisotropies. Different modes of compression and rarefication develop at the speed of sound in the plasma [16]. This tug of war, referred to as acoustic oscillations, continues until the universe becomes electrically neutral.

2 Recombination

This event is called recombination and happens at a redshift of $z = 1090$, approximately 380,000 years after the big bang [17]. The event defines a veil at the edge of our horizon, sometimes referred to as the last scattering surface. The universe now becomes comparatively transparent to light and the photons stream freely in every direction with a fraction bombarding our telescopes today. These are the CMB photons, and they carry with them information about the fundamental oscillation modes at the time of recombination.

Prior to recombination, photons and baryons are tightly coupled. Photons scatter off electrons and hydrogen atoms are quickly split apart

$$\gamma + e^- \longrightarrow \gamma + e^- \tag{4}$$

$$H + \gamma \longleftrightarrow p + e^- \tag{5}$$

As photon density and energy decreases, equilibrium is broken. Specifically when $E_\gamma < 13.6\,\mathrm{eV}$. Photons can no longer ionize hydrogen and the above relation can

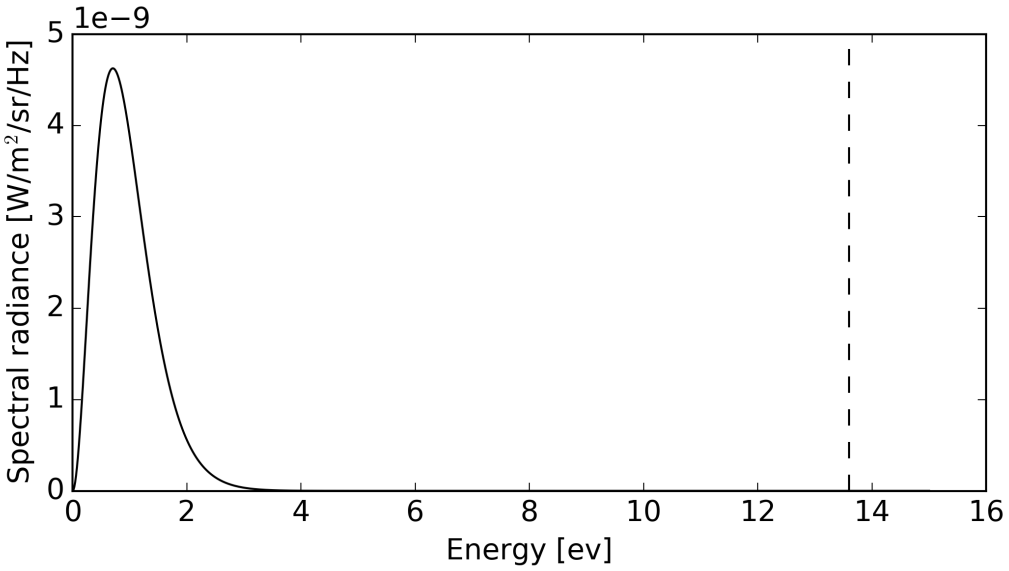

Figure 2: The spectral radiance of a blackbody with temperature $T = 3000\,K$. The tail of the photon spectral radiance distribution exceeds the ground state energy of the hydrogen atom, 13.6 eV.

only go in one direction, i.e. $\longleftrightarrow \Rightarrow \longrightarrow$.

Meanwhile, the universe is expanding and therefore the characteristic energy of the photons is redshifted. With time, the hydrogen dissociation rate also falls, and electrons and protons combine to form neutral hydrogen. As we learned in quantum mechanics, the ground state energy of the hydrogen atom is 13.6 eV. However, the photon number density is significantly greater than baryon number density (see Figure 2).

2.1 Order of Magnitude Calculations

This section from Rahman Amanullah 2015 lecture notes.

We can do an order of magnitude estimation to determine at what temperature and when this happens. The temperature today ($z = 0$) is $T_0 \approx 2.73$. The Stefan-Boltzmann relation tells us that the total radiation energy density today is given

as

$$\rho_\gamma^0 = \sigma_0 T_0^4 = 0.25\,\mathrm{eV/cm^3} \tag{6}$$

with $\sigma_0 = 4.7 \times 10^{-3}\,\mathrm{ev/cm^3/K^4}$. Similarly, we have

$$\rho_{\mathrm{crit}}^0 = \frac{3H_0^2}{8\pi G} \approx 10^4\,\mathrm{eV/cm^3}, \tag{7}$$

which suggests that $\Omega_\gamma \approx 10^{-5}$. In other words, photons only make up a tiny fraction of total energy density today. We have shown that one can write (see Chapter 4 in B&G)

$$\rho_M = \rho_M^0 (1+z)^3, \tag{8}$$

$$\rho_\gamma = \rho_\gamma^0 (1+z)^4. \tag{9}$$

Comparing the two equations above, we find that $\rho_M \approx \rho_\gamma$ happens when

$$(1+z_{\mathrm{eq}}) \approx \frac{\rho_M^0}{\rho_\gamma^0} \approx 10^4. \tag{10}$$

Here, z_{eq} represents the epoch of matter-radiation equality. The recombination event, however, happens long after matter-radiation equality. To explain this, we note that the number density of photons relative to protons during recombination is very large

$$\frac{n_\gamma}{n_H} \approx \frac{\rho_\gamma/E_\gamma}{\rho_M/m_H} \approx \frac{m_H}{E_\gamma} \approx \frac{1\,\mathrm{GeV}}{1\,\mathrm{eV}} \approx 10^9. \tag{11}$$

Here, $E_\gamma = (1+z_{\mathrm{eq}})E_\gamma^0 \sim 1\,\mathrm{eV}$, i.e., the temperature at $z = z_{\mathrm{eq}}$, and the hydrogen energy at this temperature is dominated by the proton mass.

Since there are more photons than baryons, recombination does not take place when the effective temperature of the universe corresponds to 13.6 eV (the hydrogen ionization energy), but rather at 0.25 eV. This can be understood from looking at the tail of the blackbody distribution (see Figure 2).

For a more robust discussion of recombination, please take a look at the discussion of Saha equations in Section 9.4 in B&G.

3 Reionization

The universe became electrically neutral at the time of recombination. However, we observe that the hydrogen in the interstellar medium is now largely ionized. This reionization of matter occurred at around redshift of $z \approx 10$, and is thought to have been sourced by ultraviolet radiation from the first luminous objects. We often say that the CMB photons last interacted with matter during recombination ($z = 1090$). However, about 5–10% of the CMB photons actually last scattered on charged particles that followed reionization.

The details of the reionization history of our universe are still very much a mystery! We hope to learn more about this time period as so-called 21-cm experiments (radio telescopes) advance. We can also learn something about reionization by studying the polarization of the CMB on the largest angular scales.

4 Homogeneity and Isotropy

Eiichiro Komatsu's lecture notes are incredibly clear. The content of this section is influenced by the structure of his lectures. Please take a look at pages 2–5 from: http://wwwmpa.mpa-garching.mpg.de/∼komatsu/cmb/lecture_NG_iucaa_2011.pdf.

Let's assume that we are interested in some location-dependent random variable, $X(\mathbf{q})$. More specifically, we are interested the so-called 2-point correlation function (also known as the covariance matrix). The 2-point correlation function is denoted as

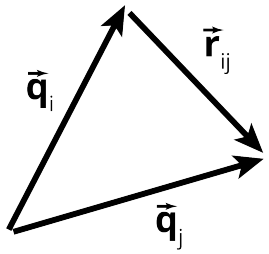

Figure 3: Vectors.

$$\xi_{ij} = \xi_{ij}(\mathbf{q}_i, \mathbf{q}_j) = \langle X(\mathbf{q}_i) X(\mathbf{q}_j) \rangle \,, \tag{12}$$

it represents the likelihood of measuring a value $X(\mathbf{q}_i)$ given a measurement at some other location $X(\mathbf{q}_j)$. Let $\mathbf{r}_{ij}$ be a vector connecting $\mathbf{q}_i$ to $\mathbf{q}_j$ (see Figure 3), then

$$\xi_{ij} = \langle X(\mathbf{q}_i) X(\mathbf{q}_i + \mathbf{r}_{ij}) \rangle \,. \tag{13}$$

Homogeneity (translational invariance) means that ξ_{ij} does not depend on the location $\mathbf{q}_i$. We should therefore be able to write

$$\xi_{ij}(\mathbf{q}_i, \mathbf{r}_{ij}) = \langle X(\mathbf{q}_i) X(\mathbf{q}_i + \mathbf{r}_{ij}) \rangle = \xi_{ij}(\mathbf{r}_{ij}) \tag{14}$$

Isotropy (rotational invariance) means that ξ_{ij} does not depend on the direction of $\mathbf{r}_{ij}$. In other words, the property that we are studying is rotational symmetric. This means that $\xi_{ij}(\mathbf{q}_i, \mathbf{r}_{ij}) = \xi_{ij}(\mathbf{q}_i, |\mathbf{r}_{ij}|)$.

By assuming homogeneity and isotropy, the 2-point correlation function therefore only depends on the magnitude of the vector connecting the two locations, $|\mathbf{r}_{ij}|$.

$$\xi_{ij}(\mathbf{q}_i, \mathbf{q}_j) = \xi_{ij}(|\mathbf{r}_{ij}|). \tag{15}$$

As far as we can tell, we live in a homogenous and isotropic universe (at least on sufficiently large scales). As the derivation above shows, when probing the statistical properties of physical quantities, invoking homogeneity and isotropy greatly simplifies the problem. We will take another look at this in Lecture 12.

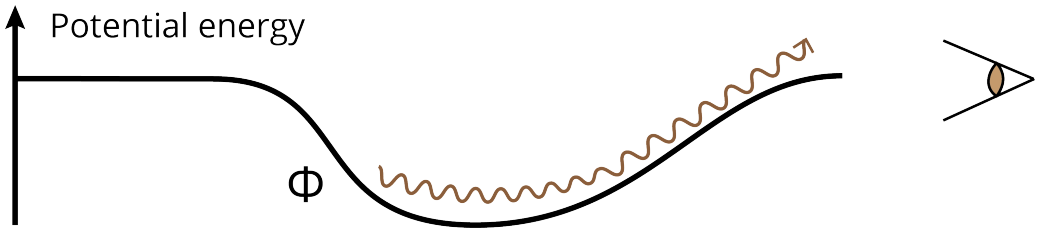

Figure 4: An illustration of the Sachs-Wolfe Effect. A photon traversing through space encounters a gravitational well characterized by a primordial density perturbation.

5 The Sachs-Wolfe Effect

Let's revisit Equation 3

$$\frac{\delta T}{T}(\mathbf{n}) = -\frac{1}{3}\Phi(\mathbf{n}).$$

This equation can be derived by looking at the geodesic equation for photons propagating in with gravitational perturbation Φ (see Lecture 3 and Chapters 3, 4, and 11 in B&G). We start by writing the temperature shift of a photon propagating through a gravitational well as

$$\left.\frac{\Delta T}{T}\right|_f = \left.\frac{\Delta T}{T}\right|_i - \Phi_i, \tag{16}$$

where i and f refer to the initial and final states. The first term on the right-hand side is the "intrinsic" temperature at early times. The second term represents the energy that is lost when a photon climbs out of a potential well.

Let's consider the case of adiabatic fluctuations in a matter dominated universe. Because we assume adiabaticity, we can safely assume that the intrinsic temperature fluctuations are proportional to the strength of the gravitational potential, in other words

$$\left.\frac{\Delta T}{T}\right|_i \sim -\Phi_i. \tag{17}$$

Adiabaticity implies that matter and radiation are perturbed in similar way and that entropy per particle is constant, regardless of whether it is a photon, baryon, or some other matter. This allows us to equate temperature and density fluctuations.

One could say that adiabaticity describes the thermal equilibrium between different energy constituents at the time when these ingredients were coupled. In other words, that the density contrast

$$\frac{\delta\rho_x}{\rho_x} \approx \frac{\delta\rho_y}{\rho_y} \tag{18}$$

regardless of what energy form x and y represent.

We want to relate initial fluctuations in the CMB temperature field to the scale factor. To achieve this, we remember that clocks run slow in a gravitational potential and that

$$ds = \sqrt{1-2\Phi}\,dt \approx (1-\Phi)dt, \tag{19}$$

with $\Phi \ll 1$. Since the temperature of the CMB is redshifting with $aT = \text{constant}$ (see Section 11.1 in B&G), we find that

$$\frac{\Delta T}{T} = -\frac{\Delta a}{a}. \tag{20}$$

We also remind ourselves that the scale factor can be linked to time according to $a(t) = t^{\frac{2}{3(1+w)}}$ which gives

$$\delta a = \frac{da}{dt}\delta t = \frac{2}{3(1+w)} t^{\frac{2}{3(1+w)}-1}\delta t, \tag{21}$$

and therefore

$$\frac{\delta a}{a} = \frac{2}{3(1+w)}\frac{\delta t}{t}. \tag{22}$$

We can now combine our results from Equations 17, 20, and 22 and find that

$$-\frac{2}{3(1+w}\frac{\delta t}{t} = -\frac{2}{3(1+w)}\Phi_i, \tag{23}$$

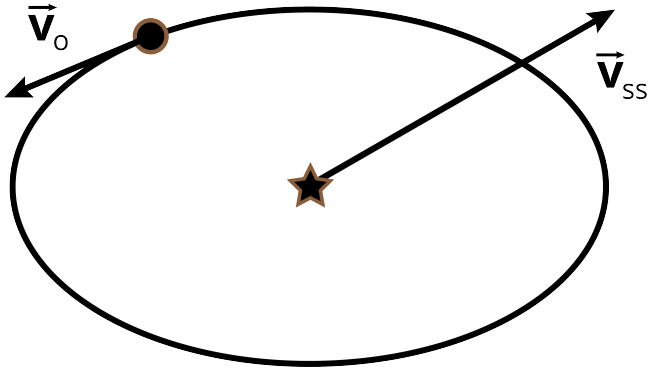

Figure 5: Our motion through space can be decomposed into motion due to our rotation around the Sun and a component that describes the overall motion of our Solar System.

which finally gives us

$$\left.\frac{\Delta T}{T}\right|_f = \frac{1+3w}{3+3w}\Phi_i. \tag{24}$$

For a matter dominated universe we have $w = 0$ which gives us Equation 3.

The Sachs-Wolfe Effect describes a contest between gravitational redshift and heating caused by local compression of matter and photons. The two effects somewhat cancel, but the net effect is that overdense regions on the sky show temperature anisotropies that are slightly cooler than average. By measuring the amplitude of the CMB temperature anisotropies, we are also constraining the amplitude of the gravitational potential variations.

6 CMB Anisotropies

6.1 The CMB Dipole

The CMB dipole is caused by our motion relative to the last scattering surface. As far as we can tell, the dipole signal can be decomposed into a component due to our motion around the sun and a component due the motion of our solar

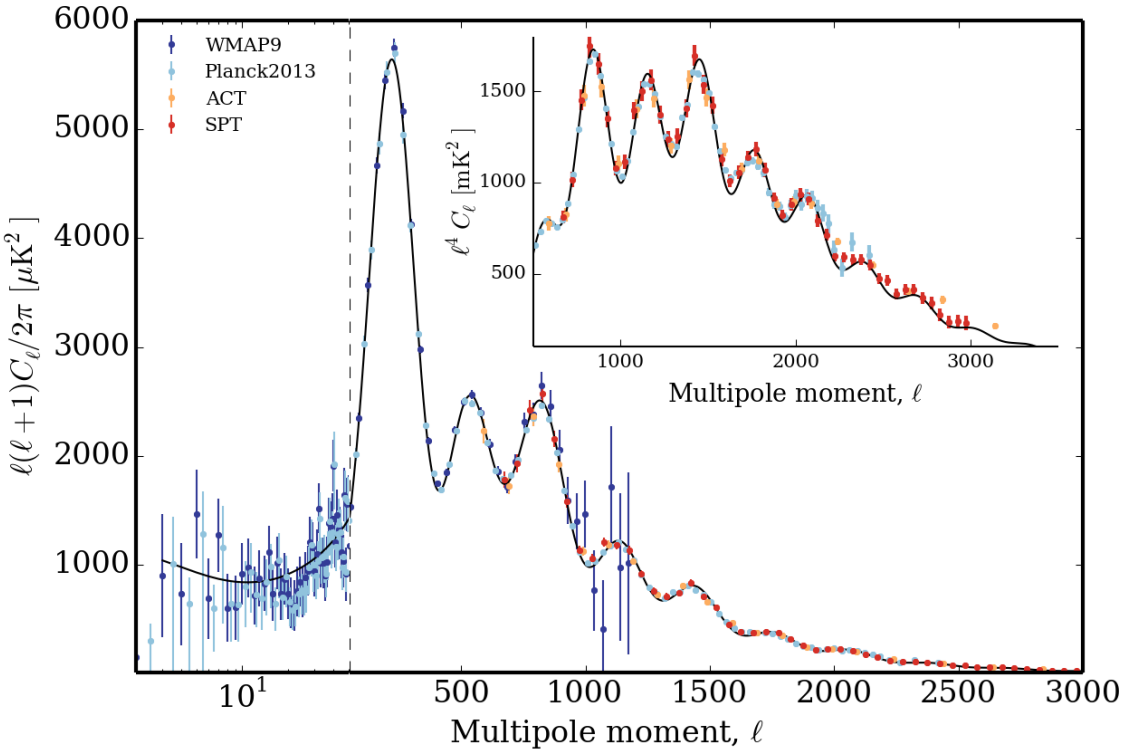

Figure 6: The temperature power spectrum from a few prominent experiments. The solid line shows the best fit power spectrum derived from *Planck* data in conjunction with polarization data from WMAP, high-ℓ experiments, and experiments measuring baryon acoustic oscillation [18]. **Inset**: The power spectrum plotted using a different scaling on the y-axis to highlight its oscillatory nature and the available measurements. The leftmost peak at $\ell \sim 800$ is the third acoustic peak. Data obtained from the Legacy Archive for Microwave Background Analysis (LAMBDA) [19].

system (see Figure 5). The amplitude of the dipole signal corresponds to about $(3355 \pm 8)\,\mu\mathrm{K}$ or about 0.1% of the amplitude of the CMB monopole. The best fit measurements suggest that our peculiar velocity is $v = 370\,\mathrm{km/s}$ in the direction $(\mathrm{lat}, \mathrm{lon}) = (264°, 48.2°)$.

6.2 Primary CMB Anisotropies

The primary CMB anisotropies correspond to $\mathcal{O}(10\,\mu\mathrm{K})$ variations in the intensity of the CMB. Outside of the Galactic plane, these anisotropies dominate the sky signal over a wide range of angular scales. The CMB anisotropies were first mapped by

the *COBE* satellite and have since then be used to obtain strong constraints on cosmological models.

The angular power spectrum has been measured by numerous experiments (see Figure 6). The *Planck* survey covered the full sky and consequently the *Planck* derived TT power spectrum estimate spans a remarkably wide ℓ-range, corresponding to angular scales of 180 degrees down to approximately 3 arcmin. In Figure 6 the acoustic oscillations can be seen as a series of peaks and throughs starting at degree angular scales, coinciding with $\ell \approx 100$. Normally the power spectra are plotted as a function of ℓ, the multipole moment. The conversion to corresponding angular scales is found by the approximate expression $\theta \approx \pi/\ell \, [\mathrm{rad}]$.

CMB temperature anisotropies, $T(\hat{\mathbf{n}}) = \delta T(\hat{\mathbf{n}})/T_0$, are naturally decomposed using spherical harmonics according to

$$T(\hat{\mathbf{n}}) = \sum_{\ell=1}^{\infty} \sum_{m=-\ell}^{\ell} a_{\ell m}^T Y_{\ell m}(\theta, \phi), \tag{25}$$

Since the spherical harmonics represent a complete function basis on the unit sphere, we should be able to decompose any square-integrable scalar function using the spherical harmonics. In other words, any function $T(\theta, \phi)$ can be written as

$$T(\theta, \phi) = \sum_{\ell=0}^{\infty} \sum_{m=-\ell}^{\ell} a_{\ell m}^T Y_{\ell}^m(\theta, \phi). \tag{26}$$

If we assume that the temperature aniostropies of the cosmic microwave background (CMB) are analytic, this expansion should therefore completely capture the information in the CMB. Now, since the spherical harmonic functions are orthogonal, we also know that

$$a_{\ell m}^T = \int d\Omega T(\theta, \phi) Y_{\ell}^m(\theta, \phi) \tag{27}$$

where the $d\Omega = \sin\theta d\theta d\phi$ integral is performed over the full area of the unit sphere. The spherical harmonic expansion of a scalar function is therefore calculated by performing an integral on the unit sphere for each function used in the expansion. We also know that since these functions are orthonormal (both orthogonal and normalized)

$$\int d\Omega Y_\ell^m(\theta,\phi) Y_{\ell'}^{m'}(\theta,\phi) = \delta_{\ell\ell'}\delta_{mm'} \tag{28}$$

Let's define the $\langle\cdot\rangle$ operator as the ensemble average defined by infinite sky realizations drawn from the same underlying theory and use this to define the correlation between spherical harmonic coefficients

$$C^{TT}_{\ell m\ell' m'} \equiv \left\langle a^T_{\ell m}\, a^{T*}_{\ell' m'}\right\rangle . \tag{29}$$

If the CMB anisotropies are homogeneous and isotropic, in other words, rotationally invariant, one can argue that

$$C^{TT}_{\ell m\ell' m'} = C^{TT}_\ell \delta_{\ell\ell'}\delta_{mm'}. \tag{30}$$

This gives

$$C^{TT}_\ell \delta_{\ell\ell'}\delta_{mm'} = \left\langle a^T_{\ell m}\, a^{T*}_{\ell' m'}\right\rangle . \tag{31}$$

So what happens when we try to find the expectation value of $T(\theta,\phi)$ over the sky? Well, we've already removed the CMB monopole from our maps (remember we're talking about the anisotropies so $\langle T(\theta,\phi)\rangle = 0$. What about the temperature anisotropy covariance?

$$\langle T(\hat{n})T(\hat{n})'\rangle = \left\langle \sum_{\ell=0}^{\infty}\sum_{m=-\ell}^{\ell} a^T_{\ell m} Y_{\ell m}(\theta,\phi) \sum_{\ell'=0}^{\infty}\sum_{m'=-\ell'}^{\ell'} a^T_{\ell' m'} Y_{\ell' m'}(\theta',\phi') \right\rangle , \tag{32}$$

$$= \left\langle \sum_{\ell=0}^{\infty}\sum_{m=-\ell}^{\ell} |a^T_{\ell m}|^2 Y_{\ell m}(\theta,\phi) Y_{\ell m}(\theta',\phi') \right\rangle . \tag{33}$$

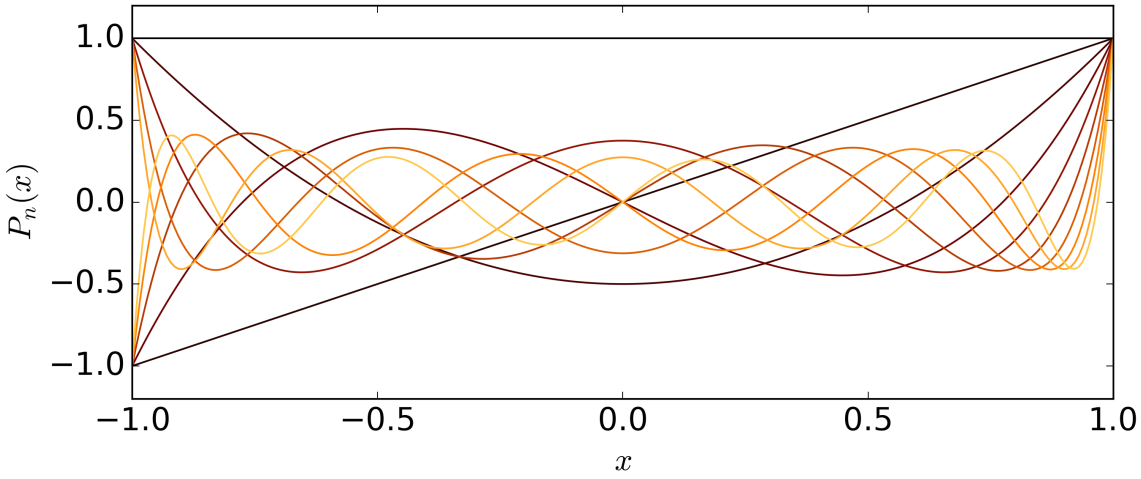

Figure 7: First 10 Legendre Polynomials.

To arrive at this expression we've assume rotational invariance to collapse the ℓ' and m' moments and simplify our expression. It follows that

$$\langle T(\hat{\mathbf{n}})T(\hat{\mathbf{n}}')\rangle = \frac{1}{4\pi}\sum_{\ell=1}^{\infty}(2\ell+1)C_\ell^{TT}P_\ell(\hat{\mathbf{n}}\cdot\hat{\mathbf{n}}'), \tag{34}$$

where $P_\ell(\hat{\mathbf{n}}\cdot\hat{\mathbf{n}}')$ is a Legendre polynomial of order ℓ and the following mathematical identity has been used (see Figure 7):

$$P_\ell(\hat{\mathbf{n}}\cdot\hat{\mathbf{n}}') = \frac{4\pi}{2\ell+1}\sum_{m=-\ell}^{\ell}Y_{\ell m}(\hat{\mathbf{n}})Y_{\ell m}(\hat{\mathbf{n}}'). \tag{35}$$

The angular power spectrum, C_ℓ^{TT}, then represents the variance in power in a given $\ell-$mode. In other words, the correlation between two points on the sphere can be represented by a series formed by the product of multipole-space power spectra and Legendre polynomials.

From all of this we have learned that the RMS temperature anisotropies associated with a particular multipole can be written as

$$\Delta T_\ell = \sqrt{\frac{\ell(\ell+1)\,C_\ell}{2\pi}}. \tag{36}$$

References

[1] Dicke, R.H. and Peebles, P.J. **Space Science Reviews**, 4: 419–460, June 1965.
[2] Peebles, P.J.E., Page, L.A. and Partridge, R.B. **Finding the Big Bang**. Cambridge University Press, Cambridge, UK, 2009.
[3] Penzias, A.A. and Wilson, R.W. **Astrophysical Journal**, 142: 419–421, July 1965.
[4] Roll, P.G. and Wilkinson, D.T. **Phys. Rev. Lett.**, 16:405–407, Mar 1966.
[5] Dicke, R.H. et al. **Astrophysical Journal**, 142:414–419, July 1965.
[6] McKellar, A. **Publications of the ASP**, 52:187, June 1940.
[7] Herzberg, G. **Molecular Spectra and Molecular Structure. Vol.1: Spectra of Diatomic Molecules**. 1950.
[8] Ohm, E.A. **Bell System Technical Journal**, 40(4):1065–1094, 1961.
[9] Jones, W.C. PhD thesis, California Institute of Technology, 2006.
[10] Fixsen, D.J. **Astrophysical Journal**, 707:916–920, December 2009.
[11] Lubin, P. et al. **Astrophysical Journal, Letters**, 298:L1–L5, November 1985.
[12] Hayakawa, S. et al. **Publications of the ASJ**, 39:941–948, 1987.
[13] Mather, J.C. et al. **Astrophysical Journal, Letters**, 354:L37–L40, May 1990.
[14] Fixsen, D.J. et al. **Astrophysical Journal**, 420:445–449, January 1994.
[15] Mather, J.C. et al. **Astrophysical Journal**, 420:439–444, January 1994.
[16] Hu, W. and White, M. **Astrophysical Journal**, 471:30, November 1996.
[17] Zel'dovich, Y.B., Kurt, V.G. and Syunyaev, R.A. **Soviet Journal of Experimental and Theoretical Physics**, 28:146, January 1969.
[18] Planck Collaboration et al. **ArXiv e-prints**, March 2013.
[19] LAMBDA. Legacy archive for microwave background analysis - web site. `http://lambda.gsfc.nasa.gov/`, May 2014.

Appendix A

The spherical harmonics represent an orthogonal function basis on the sphere. This means that any analytic scalar function, $\tau(\theta, \phi)$, can be described by the series:

$$\tau(\theta, \phi) = \sum_{\ell,m} a_{\ell m} Y_\ell^m(\theta, \phi) \tag{37}$$

What do the $Y_\ell^m(\theta, \phi)$ functions look like? Before we answer that question, let's see where these functions originate. The spherical harmonic functions are the solutions to Laplace's equation on the sphere.

$$\nabla^2 f = 0 \tag{38}$$

Harmonic functions are twice continuously differentiable functions that satisfy Laplace's equation. The etymology of the word harmonic refers to the motion of a string fixed at both ends. The solution to the differential equation for the type of motion that the string undergoes can be written as a series of sine and cosine functions.

In spherical coordinates this equation becomes

$$\nabla^2 f = \frac{1}{r^2}\frac{\partial}{\partial r}\left(r^2\frac{\partial f}{\partial r}\right) + \frac{1}{r^2\sin\theta}\frac{\partial}{\partial\theta}\left(\sin\theta\frac{\partial f}{\partial\theta}\right) + \frac{1}{r^2\sin^2\theta}\frac{\partial^2 f}{\partial\phi^2} = 0 \qquad (39)$$

Remember that all harmonic functions are analytic. This means that the functions can be locally represented by a convergent power series which in turn means that the harmonic functions are infinitely differentiable.

As so often in PDE's we explore solutions that allow for separation of variables. The function that describes the θ and ϕ dependence of the solution (imagine we've fixed r) is

$$Y_\ell^m(\theta,\phi) = (-1)^m\sqrt{\frac{(2\ell+1)}{4\pi}\frac{(\ell-m)!}{(\ell+m)!}}e^{im\phi}P_\ell^m(\cos\theta) \qquad (40)$$

where we've picked a normalization factor that makes Y_ℓ^m orthonormal. The associated Legendre polynomials, P_ℓ^m, are the canonical solutions of the general Legendre equation

$$(1-x^2)\frac{d^2}{dx^2}P_\ell^m(x) - 2x\frac{d}{dx}P_\ell^m(x) + \left[\ell(\ell+1) - \frac{m^2}{1-x^2}\right]P_\ell^m(x) \qquad (41)$$

From the above equation, we see that the spherical harmonics functions are inextricably bound to the associated Legendre polynomials, P_ℓ^m.